Cell division in a minimal bacterium in the absence of ftsZ

Maria Lluch-Senar, Enrique Querol, Jaume Piñol

molecular microbiology

Cell division in a minimal bacterium in the absence of ftsZ

Journal:	*Molecular Microbiology*
Manuscript ID:	MMI-2009-09676.R2
Manuscript Type:	Research Article
Date Submitted by the Author:	09-Jul-2010
Complete List of Authors:	Lluch-Senar, Maria; Universitat Autònoma de Barcelona, Bioquímica i Biologia Molecular Querol, Enrique; Universitat Autònoma de Barcelona, Bioquímica i Biologia Molecular Piñol, Jaume; Universitat Autònoma de Barcelona, Institut de Biotecnologia i Biomedicina and Departament de Bioquímica i Biologia Molecular
Key Words:	Mycoplasma genitalium , cell division, ftsZ, gliding motility

Cell division in a minimal bacterium in the absence of *ftsZ*

Maria Lluch-Senar, Enrique Querol and Jaume Piñol*

Institut de Biotecnologia i Biomedicina and Departament de Bioquímica i Biologia Molecular. Universitat Autònoma de Barcelona, 08193 Bellaterra, Barcelona, Spain.

***Corresponding author:**

Jaume Piñol

Phone: 34-93-5811278

Fax: 34-93-5812011

E-mail: jaume.pinyol@uab.cat

Running title: *ftsZ* and cell division in *M. genitalium*

Key words: *Mycoplasma genitalium, ftsZ*, cell division, gliding motility

ABSTRACT

Mycoplasma genomes exhibit an impressively low amount of genes involved in cell division and some species even lack the *ftsZ* gene, which is found widespread in the microbial world and is considered essential for cell division by binary fission. We constructed a *Mycoplasma genitalium ftsZ* null mutant by gene replacement to investigate the role of this gene and the presence of alternative cell division mechanisms in this minimal bacterium. Our results demonstrate that *ftsZ* is non-essential for cell growth and reveal that, in the absence of the FtsZ protein, *M. genitalium* can manage feasible cell divisions and cytokinesis using the force generated by its motile machinery. This is an alternative mechanism, completely independent of the FtsZ protein, to perform cell division by binary fission in a microorganism. We also propose that the mycoplasma cytoskeleton, a complex network of proteins involved in many aspects of the biology of these microorganisms, may have taken over the function of many genes involved in cell division, allowing their loss in the regressive evolution of the streamlined mycoplasma genomes.

INTRODUCTION

Mycoplasmas are characterized by having small genomes with a low G+C content and by the absence of a cell wall, which confers on them a pleomorphic appearance. These microorganisms, belonging to the *Mollicutes* class, are widespread in nature and they are parasites or pathogens of a very broad range of hosts, including humans. Although they have a minute and deceptively simple appearance, a closer study of mycoplasma cells reveals considerable intricacy. Despite their reduced genomes, many mycoplasmas have advanced systems required for a parasitic life such as adhesion and internalization inside host cells, antigenic variation, extensive membrane transport systems, or the ability to locomote over solid surfaces (gliding motility).

Mycoplasma genitalium is considered the etiological agent of non-gonococcal and non-chlamydial urethritis (Jensen, 2004). The most relevant structure in the *M. genitalium* cytoplasm is a cytoskeleton organized around a rod shaped electrondense core (Hatchel and Balish, 2008; Pich *et al.*, 2008) that defines a distinctive tip structure known as terminal organelle. The majority of cytoskeletal proteins present in the terminal organelle have been primarily identified as cytadhesins or cytadherence-associated proteins (Burgos *et al.*, 2006; Burgos *et al.*, 2007; Pich *et al.*, 2008). However, a variety of proteins involved in energy metabolism (dihydrofolate reductase, DHFR), translation/transcription (Elongation factor Tu), heat shock (DnaK), and cell division (FtsZ) were also identified as cytoskeletal proteins in the closely related species *Mycoplasma pneumoniae* (Regula *et al.*, 2001). The terminal organelle is essential for cytadherence and further parasitism of host target cells (Burgos *et al.*, 2006; Mernaugh *et al.*, 1993) and has a key role in the guidance of the mycoplasma movement (Burgos *et al.*, 2008). Compelling evidence also support that the terminal organelle is (or

contains) the molecular motor for gliding motility in *M. pneumoniae* (Hasselbring and Krause, 2007).

Untreated *M. genitalium* infections can persist for a long time (Cohen *et al.*, 2007; Hjorth *et al.*, 2006). Among the mechanisms allowing for such persistence, there are highly sophisticated systems to evade the host immune response. The most obvious one is probably the intracellular residence of this microorganism, but mechanisms to generate antigenic variation can also be found. It is well known that variability occurs in the P140 and P110 main adhesins, which are essential for the terminal organelle development (Burgos *et al.*, 2006). These adhesins are encoded, respectively, by ORFs *mg191* and *mg192* (also referred to as *mgpB* and *mgpC*), located inside the MgPa operon. Several non-coding sequences reminiscent of *mg191* and *mg192* also exist, scattered along the *M. genitalium* genome, and they are known as MgPa repeats or MgPa islands (Fraser *et al.*, 1995; Peterson *et al.*, 1995). Prominent in a densely packed genome of only 580 kb, these repetitive sequences provide a nearly unlimited source of antigenic variation by recombining amongst themselves and with the coding sequences in the MgPa operon (Iverson-Cabral *et al.*, 2007; Ma *et al.*, 2007). MgPa islands also endow a phase variation mechanism which can switch ON-OFF, in a reversible or irreversible way, the expression of P110 and P140 adhesins (Burgos *et al.*, 2006). These phase variants are also generated by recombination and they lose the terminal organelle, in consequence being unable to adhere to host cells or other surfaces.

It is currently thought that mycoplasmas evolved from bacteria of the *Firmicutes* taxon by regressive evolution (Weisburg *et al.*, 1989). A parasitic way of life in very constant environments likely led ancient mycoplasmas to lose many of their genes, in this way

modeling the minimal genomes that these microorganisms exhibit. One of the clearest examples of such reductive evolution can be seen when examining the operons or clusters containing genes involved in cell division. While it is very common to find 15 or 16 genes in the division and cell wall synthesis cluster (DCW) of cell-walled bacteria, most sequenced mycoplasma genomes include only *mraZ*, *mraW*, *ftsZ* and one gene encoding a hypothetical protein. It is also noteworthy that some mycoplasma species may even lack several of these genes. Despite the fact that a few other genes may also be collaborating in cell division (Alarcón *et al.*, 2007), genes in the DCW of mycoplasmas are expected to be essential for cell growth. This view was reinforced when no disruptions were identified in the corresponding operons of *M. genitalium, M. pneumoniae* and *M. pulmonis* by global transposon mutagenesis (French *et al.*, 2008; Glass *et al.*, 2006; Hutchison *et al.*, 1999). However, in a previous work we found a transposon insertion inside the coding region of *M. genitalium ftsZ* (Lluch-Senar *et al.*, 2007). This gene was shown to be transcribed in *M. genitalium* (Benders *et al.*, 2005) and is considered essential for cell division by binary fission. The encoded tubulin-like FtsZ protein is the first component of the cell division apparatus that arrives at the division site and polymerizes at midcell, forming a filamentous ring (Z-ring) that recruits additional proteins required for the progression and the completion of cytokinesis (Weiss, 2004).

The transposon insertion previously identified in *ftsZ* was compatible with the presence of a truncated protein containing a significant amount (40%) of the amino acid sequence. Thus, we aimed to construct a *M. genitalium ftsZ* null mutant by gene replacement to better understand the role of this protein. The obtained mutant strain was characterized in terms of growth kinetics, ultrastructure, cell adhesion and gliding

motility. The results confirm our previous expectations indicating a non-essential role of *ftsZ* for cell growth and reveal that, in the absence of the FtsZ protein, *M. genitalium* can still manage a feasible cell division and cytokinesis using the force generated by the gliding motility apparatus. To our knowledge, this is the first report depicting alternative mechanisms to perform cell division by binary fission in a microorganism that already contains the *ftsZ* gene.

RESULTS

Obtaining a *M. genitalium ftsZ* null mutant

M. genitalium ftsZ (ORF *mg224)* was deleted by gene replacement. The pΔftsZ*Tet* suicide plasmid was designed to contain the *tetM438* selectable marker enclosed by the flanking regions of the *mg224* ORF (Fig. 1A). After transforming *M. genitalium* wild-type (WT) G37 strain with plasmid pΔftsZ*Tet*, recombinant clones were analyzed by Southern blot (Fig. 1B). Two of ten clones showed the intended replacement as a result of a double-crossover recombination event between pΔftsZ*Tet* and the mycoplasma genome, resulting in the complete deletion of the *mg224* ORF (Fig. 1A). The absence of *ftsZ* in the null mutants, which were termed Δ*ftsZ*, was also confirmed by PCR and Southern blot (Fig. 1C, E). Importantly, plasmid pΔftsZ*Tet* was designed to preserve promoter signals surrounding the *mg224* ORF (Fig. 1A), in particular the previously identified promoter sequence upstream of *mg225* ORF (Benders *et al.*, 2005). To confirm that the deletion in *ftsZ* was not affecting the transcription of downstream genes, cDNA from *mg225* ORF in Δ*ftsZ* mutants was consistently amplified by RT-PCR (Fig. 1D).

Growth kinetics of Δ*ftsZ* cells

The growth kinetics of the Δ*ftsZ* mutant was compared to that of the WT strain. The cell mass from several cultures of both strains was measured by ATP luminometry (Lluch-Senar *et al.*, 2007; Stemke, 1995). Cultures of both strains exhibited the same doubling time in log phase (11.8 h and 11.7 h, respectively) and no significant differences were found when analyzing additional parameters such as the cell mass in the stationary phase. These results indicate that cells not only remain viable upon deletion of *ftsZ*, but also that this deletion has no impact on growth kinetics of *M. genitalium*.

Adhesion properties and cytoskeletal structure of Δ*ftsZ* cells

Since FtsZ protein has previously been identified as a cytoskeletal protein in the related species *M. pneumoniae* (Regula *et al.*, 2001), we were prompted to investigate the presence of defects in the adherence properties as well as downstream events affecting other cytoskeletal proteins in Δ*ftsZ* mutants. Haemadsorption (HA) was qualitatively assessed, and colonies from Δ*ftsZ* cells exhibited the same HA^+ phenotype as colonies from WT cells. Δ*ftsZ* cells did not show significant differences regarding their plastic adhesion properties (Table 1). Neither were there significant differences found when examining the protein profiles of Δ*ftsZ* and WT cells by SDS-PAGE and Western blot. In particular, Δ*ftsZ* cells exhibited WT levels of MG386, HMW1, HMW2, P140, P110, HMW3 and P41 proteins (data not shown), indicating that deletion of *ftsZ* does not give rise to detectable downstream events in most of the cytoskeletal proteins of *M. genitalium*. In addition, examination of ultrathin sections of Δ*ftsZ* cells by transmission electron microscopy did not reveal appreciable ultrastructural changes in the electrondense core or other cytoskeletal components of the terminal organelle. However, long cell extensions were frequently observed in the pole opposite to the terminal organelle of Δ*ftsZ* cells (Fig. 3A).

Gliding motility properties of Δ*ftsZ* cells

Because no significant changes were observed in the cytoskeleton of the mutant cells, no changes were expected in the gliding motility properties of Δ*ftsZ* cells. However, gliding motility was assessed by examining colony morphology in culture dishes covered with semisolid medium. Under these conditions, colonies from cells with gliding motility defects are compact and do not exhibit the microsatellite colonies that are typically developed from gliding proficient cells (Pich *et al.*, 2006a). Surprisingly, colonies from Δ*ftsZ* cells were more compact and with fewer satellite microcolonies than those from WT cells (Fig. 3B), suggesting that deletion of *ftsZ* interferes in some way with the gliding motion. Gliding motility was also monitored by microcinematography. The speed and movement patterns of Δ*ftsZ* cells were essentially the same shown by WT cells, although it was noticeable that 39% of Δ*ftsZ* cells vs. 10% of WT cells remained non-motile during the observation period (Table 1). Interestingly, in the microcinematographies most non-motile Δ*ftsZ* cells were found very close to another non-motile cell, and sometimes both cells seemed to be linked by a thin filament (Fig. 3C). Thus, the high ratio of non-motile Δ*ftsZ* cells is consistent with the more compact phenotype of the colonies of this strain. However, the normal velocity and movement patterns exhibited by motile Δ*ftsZ* cells suggest that the FtsZ protein is not directly involved in the gliding mechanics of mycoplasma.

Analysis of dividing Δ*ftsZ* cells

To investigate the origin of non-motile cells detected in the Δ*ftsZ* strain, the mutant strain was analyzed by scanning electron microscopy (SEM). The images confirmed the presence of a large number of coupled cells linked by a thin filament (Fig. 4A and B) that were also observed in pictures from the cinematographies. Noteworthy, these

coupled cells exhibited terminal organelles at both ends. Since the terminal organelle is the leading end in the mycoplasma motion (Bredt, 1968; Burgos *et al.*, 2008), cells bearing two terminal organelles in the same direction but opposite senses are expected to be non-motile or barely motile. The images also suggest that these cells are dividing cells in the latter stages of cytokinesis, as has recently been demonstrated in *M. pneumoniae* (Hasselbring *et al.*, 2006a). In addition, cells exhibiting a long tail in the pole opposite of the terminal organelle as well as chains of cells were also very common (Fig. 4A and B). Such morphologies were rarely observed when examining WT cells and are in agreement with the possibility that the force generated by the gliding motility apparatus in one or both daughter cells may be strong enough to separate dividing Δ*ftsZ* cells.

Introducing non-adherent mutations in the Δ*ftsZ* strain

If the gliding apparatus is essential for cytokinesis in Δ*ftsZ* cells, additional mutations abolishing motility in this strain should render cells unable to divide, thus being, in consequence, non-viable. Unfortunately, methods to construct strains bearing conditional lethal mutations are not currently available in mycoplasmas. However, we have taken advantage of the phase variation mechanism that deletes a region involving coding sequences of P110 and P140 adhesins (Burgos *et al.*, 2006) to investigate the role of the gliding machinery in the cytokinesis of Δ*ftsZ* cells. Since P140 and P110 proteins are required for cell adhesion, phase variants are also expected to be non-motile. Supporting this view, *M. pneumoniae* cells are non-motile after disruption of the gene coding for the P1 adhesin (Hasselbring *et al.*, 2006b), homologous to the P140 adhesin. In addition, phase variants occur with high frequency in the WT strain and can

213 be easily detected. Therefore, if gliding motility is essential for cell division in the
214 absence of *ftsZ*, no phase variants should be detected among cells of the Δ*ftsZ* strain.
215
216 Based on this rationale, the presence of HA$^-$ variants in serial culture passages of WT
217 and Δ*ftsZ* strains was screened. Viable, non-adherent cells were detected when they
218 were able to develop HA$^-$ colonies on agar plates (Mernaugh *et al.*, 1993). The
219 frequency of phase variants was low at passage 0 of WT cultures (0.3%) but it increased
220 rapidly until becoming stabilized with a frequency of around 2.8% in the last passages
221 (Fig. 5A and B). In contrast, phase variants were never detected in the successive
222 culture passages of the Δ*ftsZ* strain. This result indicates that HA$^-$ phase variants are not
223 viable in the genetic background of the Δ*ftsZ* strain. The presence of the recombinant
224 chromosomes from phase variants in the serial culture passages was also investigated.
225 For this purpose, a quantitative real time PCR (Q-PCR) was designed to detect a
226 specific amplicon resulting from the recombination of the MgPa operon with MgPa
227 island VI (Fig. 5C and D). Detection of this amplicon only reveals the presence of
228 chromosomes from a fraction of non-adherent cells since additional recombination
229 events rendering non-adherent cells are also possible with other MgPa islands (Burgos
230 *et al.*, 2006). The identity of this amplicon was confirmed by sequencing (data not
231 shown). At passage 0, the frequency of recombinant chromosomes was very similar in
232 the cultures from both strains (0.1%). This result indicates that recombination events
233 deleting a portion of the MgPa operon also occur in the Δ*ftsZ* strain and these events
234 have a similar frequency in the WT strain. In WT cultures, the frequency of
235 chromosomes with a deletion in the MgPa operon was progressively increased until
236 reaching values close to 0.4% in the fourth passage and then remained stabilized until
237 the end of the experiment (Fig. 5C). Cultures from the Δ*ftsZ* strain did not show such

238 increase in the number of recombinant chromosomes, indicating that cells bearing a
239 deletion in the MgPa operon do not accumulate along the serial passages and mutations
240 rendering non-adherent cells are lethal in the Δ*ftsZ* strain**.**
241
242 **Complementation analysis of the Δ*ftsZ* strain**
243 Because only two Δ*ftsZ* mutants were isolated by gene replacement, a complementation
244 assay of the Δ*ftsZ* strain was performed to exclude the presence of additional genetic
245 defects in this strain. The WT *ftsZ* allele under the control of the *mg438* constitutive
246 promoter (Burgos *et al.*, 2007) was reintroduced by transposition to Δ*ftsZ* cells by using
247 plasmid pTnG*ftsZ* (Table S2). After transforming with this plasmid, 58% of the
248 recovered colonies exhibited normal growth, with the presence of a large number of
249 microsatellites (Fig S1), suggesting that the WT *ftsZ* allele in Δ*ftsZ* cells was able to
250 restore the normal gliding phenotype. Four colonies were picked, filtered-cloned and the
251 corresponding cultures were analyzed by Southern blot to exclude the presence of
252 multiple transposon insertions (data not shown). Microcinematographies from cells of
253 two of these colonies confirmed that gliding motility parameters were restored to
254 normal levels (Fig. S1). In the same way, SEM analyses demonstrated that frequencies
255 of different morphologies were restored to values very close to those shown by WT
256 cells (Fig. 4A). Finally, one of these transformants was submitted to successive
257 passages and HA^- phase variants were recovered again, with a very similar frequency to
258 that observed in the WT strain (Fig. S1). Together, these data indicate that the presence
259 of the WT *ftsZ* allele is able to restore the normal growth parameters in Δ*ftsZ* cells, and
260 exclude that genetic defects other than the absence of *ftsZ* are involved in the phenotype
261 exhibited by the Δ*ftsZ* strain.
262

DISCUSSION

The sequencing of mycoplasma genomes has revealed the presence of few genes orthologous to those involved in cell division of most cell-walled bacteria. Although genes involved in the segregation of the peptidoglycan layer are obviously useless in mycoplasmas, it is perplexing to see how these microorganisms can divide by binary fission in the absence of several genes crucial for the Z-ring architecture. Moreover, the absence of these genes is difficult to explain, since their function cannot be rescued simply by uploading external cell resources, as is the case of genes involved in metabolism, and suggests the existence of alternative mechanisms in the cell division of these microorganisms. The previous isolation of a *ftsZ* transposon generated mutant prompted us to characterize the role of this gene and the encoded protein in *M. genitalium* in depth and thus gain insight into its biology and cell division systems. The data reported herein demonstrate that *M. genitalium* cells can divide by binary fission in the absence of FtsZ and highlight the role of the terminal organelle and its associated cytoskeletal structures in the cell division of this minimal microorganism. This finding is comparable to the L-forms of *Bacillus subtilis* dividing by a "budding" or "extrusion-resolution" mechanism in the absence of the *ftsZ* gene, probably reflecting the presence of ancient proliferative mechanisms in the modern microorganisms (Leaver *et al.*, 2009). Our results suggest that in *M. genitalium* binary fission may be accomplished by two redundant mechanisms, the first one based on the well-known *ftsZ* machinery and the second one based on the pivotal roles of the mycoplasma cytoskeleton and gliding motility.

FtsZ has previously been identified as a component of the cytoskeletal fraction of *M. pneumoniae* cells (Regula *et al.*, 2001), in accordance with the biochemical properties

of eukaryotic cytoskeletal tubulins (Ramsby and Makovsky, 1999). Nonetheless, cells from the Δ*ftsZ* strain do not exhibit adherence defects or detectable changes in their cytoskeletal ultrastructure and glide at the same velocity as do WT cells. Furthermore, Δ*ftsZ* cells do not show downstream events in their levels of proteins involved in cell adhesion and motility. These functional impairments and such downstream events are commonly observed in strains with deletions or disruptions in genes coding for functional cytoskeletal proteins in *M. genitalium* (Burgos *et al.*, 2006; Burgos *et al.*, 2008; Pich *et al.*, 2008) and *M. pneumonaie* (Krause and Balish, 2001). While our results do not discard the possible association of FtsZ with the main structures of the mycoplasma cytoskeleton, they exclude a role for this protein in the functions traditionally linked to the terminal organelle and its associated cytoskeletal structures.

SEM analysis of the Δ*ftsZ* strain reveals a high frequency of mutant cells in the latter stages of cytokinesis, suggesting that this process takes a long time in this strain (approximately four hours). In contrast, the low frequency of dividing cells that can be observed when examining the WT population indicates that cytokinesis is a process that can be accomplished in one hour and suggests that most of non-dividing cells are motile. Nevertheless, the long time spent to segregate dividing Δ*ftsZ* cells has no impact in the overall duration of the cell cycle in *M. genitalium* since doubling times are very similar in both strains, suggesting that the temporal control of the cell cycle in mycoplasmas is independent of the length of cytokinesis. This is in contrast with previous observations indicating the presence of specific checkpoints controlling the cell cycle of *Caulobacter crescentus* (Hottes *et al*., 2005; Jensen, 2006; Shen *et al*., 2008). Alternatively, the time between two consecutive division rounds in *M.*

312 *genitalium* may be long enough to provide a significant buffering capacity in the case of
313 a delay in the cytokinesis, as has been observed in the Δ*ftsZ* cells.
314
315 We have provided evidence that mutations rendering non-adherent cells might be lethal
316 in the Δ*ftsZ* strain. This was demonstrated by quantifying the appearance of viable non-
317 adherent phase variants and chromosomes with deletions in the MgPa operon along
318 serial culture passages. In these experiments, the frequency of non-adherent phase
319 variants was very low in the first passages of WT cultures. This result can be explained
320 by the fact that only collected cells growing attached to the plastic surface of culture
321 flasks from routine cultures of *M. genitalium* WT cells were collected, thus avoiding the
322 accumulation of non-adherent cells in the laboratory stocks. Since both adherent and
323 non-adherent cells were used to start the next serial passages, the frequency of non-
324 adherent cells progressively increased, reaching values close to 3%. This frequency is
325 high enough to allow the detection of phase variants among the Δ*ftsZ* cell population if
326 such non-adherent cells are viable. In the same way, recombinant chromosomes bearing
327 deletions in the MgPa operon do not accumulate in the successive serial passages,
328 supporting that HA^- phase variants are not viable in Δ*ftsZ* cultures. Furthermore, SEM
329 images suggest that the long tails in the mutant strain are produced as a consequence of
330 the force generated by the gliding motility apparatus in the absence of FtsZ. Such tails
331 become progressively longer and thinner until they are eventually broken. Taken
332 together, these results strongly suggest that gliding motility is essential to segregate
333 dividing Δ*ftsZ* cells. However, such broken tails have to be rapidly resealed to maintain
334 cell integrity. Because Δ*ftsZ* cells grow at the same rate as WT cells, these data suggest
335 that the mycoplasma cell membrane is very efficient when sealing such broken ends. A
336 similar conclusion can be drawn from a previous work showing that terminal organelles

may detach from the main cell body of *M. pneumoniae* cells deficient for P41 (Hasselbring and Krause, 2007).

Mycoplasmas lack genes coding for Min and SlmA or Noc proteins. These proteins, especially the Min group, have a very important role as negative effectors of FtsZ polymerization and are essential for the establishment of cell polarity and the correct placement of the division site at midcell. SlmA and Noc proteins provide a second mechanism, the nucleoid occlusion system, to prevent the formation of septa over nucleoids (Rothfield *et al.*, 2005). On the other hand, *M. genitalium* strains with deletions in *mg191* or *mg192* lose the terminal organelle and exhibit a high frequency of cells of variable size and cells with a multilobed or a pleomorphic appearance, indicating the presence of defects in their cell division process (Burgos *et al.*, 2006). Preliminary work also indicates the existence of dramatic changes in the electrondense core ultrastructure of the cells from those strains, thus suggesting a role for cytoskeleton in the cell division of *M. genitalium* (Burgos *et al.*, unpublished data). Because the cytoskeleton is the most notable polar component of this microorganism, this structure may also be involved in the placement of the Z-ring in WT cells. Therefore, the presence of a cytoskeleton in many mycoplasma species can also be seen as an opportunity to undertake many of the functions of cell division proteins missing in mycoplasmas.

One open question finally arises. If *ftsZ* is not essential for cell division in mycoplasma, why is this gene still present in the streamlined genome of *M. genitalium*? As is shown here, dividing Δ*ftsZ* cells remain fixed at the same location for extended periods of time. Such lengthy time in the absence of movement may be detrimental for the *in vivo*

survival of this mycoplasma, in this way providing a selective pressure against the loss of this gene. However, alternative explanations may also be possible, since dividing cells of *M. pneumoniae*, a related respiratory mucosal pathogen, can remain non-motile for several hours (Hasselbring *et al*., 2006a) despite the presence of a functional *ftsZ*. We suggest an alternative possibility, related to the intracellular residence of *M. genitalium*, also favoring the conservation of this gene. Soon after the internalization of *M. genitalium* inside eukaryotic host cells, mycoplasmas appear enclosed in vacuoles, many of them with a perinuclear location (Jensen *et al*., 1994; McGowin *et al*., 2009; Mernaugh *et al*., 1993). Since one of the prerequisites for gliding motility is the presence of a solid surface, it is plausible to think that the gliding force can be ineffective to support cell division in internalized mycoplasmas. In this scenario, *ftsZ* should be essential for the intracellular survival of *M. genitalium*. Fortunately, this hypothesis is fully testable and may reveal a new role for *ftsZ* as a virulence factor of mycoplasmas.

EXPERIMENTAL PROCEDURES

Bacterial strains and growth conditions. *Escherichia coli* strain XL-1 Blue was grown at 37 ºC in 2YT broth or LB agar plates containing 75 µg ml^{-1} ampicillin, 40 µg ml^{-1} X-Gal and 24 µg ml^{-1} Isopropyl-beta-thio galactopyranoside (IPTG) when needed. The *M. genitalium* G-37 WT strain was grown in SP-4 medium (Tully *et al*., 1979) at 37 ºC under 5% CO_2 in tissue culture flasks (TPP). To select the pΔftsZ*Tet M. genitalium* transformant cells, plates were supplemented with 2 µg ml^{-1} tetracycline. To select pTnG*ftsZ* complemented cells (TnG*ftsZ* strain), plates were supplemented with 2 µg ml^{-1} tetracycline and 100 µg ml^{-1} gentamicin.

DNA manipulations. DNA genomic of *M. genitalium* was isolated by using the E.Z.N.A. Bacterial DNA Kit (Omega BIO-TEK). Plasmidic DNA was obtained by using the Fast Plasmid Mini Eppendorf Kit. All primers and plasmids used in this work are summarized in Tables S1 and S2. The purification of PCR products and digested fragments from agarose gels was achieved using the E.Z.N.A. Gel Extraction Kit (Omega BIO-TEK).

Molecular cloning. A 1-kb PCR fragment encompassing the upstream region of *mg224* was obtained by using primers 5'BEΔftsZ and 3'BEΔftsZ, which contain the *Pst*I and *Eco*RI restriction sites, respectively, at their 5' ends. Another 1-kb PCR fragment encompassing the downstream region of *mg224* was obtained by using primers 5'BDΔftsZ and 3'BDΔftsZ that contain, at their ends, the *Bam*HI and *Cla*I restriction sites, respectively. Both PCR fragments were cloned into *Eco*RV-digested pBE (Pich *et al.*, 2006b), excised with the corresponding enzymes (Roche), and ligated together with a 2-kb *Bam*HI-*Eco*RI fragment encompassing the *tetM438* selectable marker (Pich *et al.*, 2006b) and a *Pst*I-*Cla*I digested pBSKII(+) (Invitrogen). This ligation mixture resulted in the p*ΔftsZTet* vector that was used to transform *M. genitalium* G-37 and obtain the *mg224* null mutant (Δ*ftsZ*). To construct the pTnG*ftsZ* plasmid, a 1.1-kb PCR fragment encompassing the *mg224 gene* was first obtained by using primers 5'TnftsZ and 3'TnftsZ. Primer 5'TnftsZ contains a *Pst*I restriction site and the promoter sequence of *M. genitalium mg438* ORF (Pich *et al.*, 2006b). Primer 3'TnftsZ contains a *Eco*RI rescticion site at its 5' end. The PCR fragment was cloned into *Eco*RV-digested pBE, excised with *Eco*RI-*Pst*I enzymes, and ligated to the pMTn*Gm Eco*RI-*Pst*I digested vector (Pich *et al.*, 2006b). The resulting vector was used to transform the Δ*ftsZ* strain as described below.

412

413 **Transformation of *M. genitalium*.** Transformation of *M. genitalium* was performed by
414 electroporation using 30 µg of DNA as previously described (Pich *et al.*, 2006b).

415

416 **Southern blotting and PCR assays.** Genomic DNA of pΔftsZ*Tet* transformants were
417 digested with *Kpn*I enzyme and hybridized as previously described (Pich *et al.*, 2006b)
418 using probe S1, which was a 1-kb fragment obtained by digesting pΔftsZ*Tet* with
419 *Pst*I/*Eco*RI restriction enzymes (Fig. 1A). Genomic DNAs of Δ*ftsZ* and WT were
420 digested with *Eco*RV and hybridized using probe S2, which was a 1.1-kb fragment
421 encomprissing *ftsZ* amplified by PCR using 5'ftsZ and 3'ftsZ primers (Fig. 1A and
422 Table S1). The Δ*ftsZ* mutants were also checked by PCR. The positive control was
423 performed by amplifying a 1-kb PCR fragment encompassing the upstream
424 region of *mg224* by using primers 5'BEΔftsZ and 3'BEΔftsZ (Table S1) and WT or
425 Δ*ftsZ* genomic DNAs as a template. To check the presence of Δ*ftsZ* mutants, a 1.1-kb
426 fragment of *ftsZ* was amplified using 5'ftsZ and 3'ftsZ primers (Table S1) and genomic
427 DNA of WT or Δ*ftsZ* as a template (Fig. 1C). Genomic DNAs of four TnG*ftsZ* mutants
428 were digested with *Eco*RV and hybridized using a probe of the gentamicin gene (data
429 not shown). PCR products were sequenced to confirm the identity of the amplified
430 fragments (data not shown).

431

432 **RNA manipulations.** Total RNA from 20 ml of mid-log phase cultures of *M.*
433 *genitalium* G-37 and Δ*ftsZTet* mutants was extracted by using the RNAaqueous kit
434 (Ambion). For RT-PCR assays, total RNA was treated with DNase I (New England
435 Biolabs), and retrotranscribed using the SuperScript first-strand synthesis system kit

436 (Invitrogen) and the 3'BDKOftsZ primer. The cDNA was amplified by PCR using the
437 5'RTmg225 and 3'BDKOftsZ primers, obtaining a fragment of 450 bp (Fig. 1D).
438
439 **Electron microscopy**. Samples were analyzed by TEM as previously described (Pich *et*
440 *al.*, 2008). Samples were analyzed by SEM according to the following procedure. Mid-
441 log phase cells grown in Lab-Tek chamber slides (Nunc) were washed three times with
442 phosphate-buffered saline (PBS) and fixed with 1% glutaraldehyde for 1 h. Samples
443 were washed three times with PBS and then dehydrated sequentially with 30%, 50%,
444 70%, 90% and 100% ethanol for 10 min each. Immediately, samples were critical point
445 dried (K850 critical point drier; Emitech Ashfort; United Kingdom) and sputter coated
446 with 20 nm thin gold layer. Samples were observed using a Hitachi S-570 (Tokyo,
447 Japan) microscope. About 500 cells from each strain were analyzed to determine the
448 frequency of cells in the different stages. The percentages of morphologies showing a
449 terminal organelle at both poles of mycoplasma cells (Fig. 4A, stages 3 and 4) were
450 used to estimate the length of cytokinesis. This length was calculated as the product of
451 the frequency of dividing cells by the doubling time derived from the slopes of growth
452 curves (see below).
453
454 **Microcinematography.** Samples with different cell densities were prepared as
455 previously described (Pich *et al*., 2006a). Cell movement was examined at 37 °C using a
456 Nikon Eclipse TE 2000-E microscope and images were captured with a Digital Sight
457 DS-SMC Nikon camera controlled by NIS-Elements BR software. Particular
458 movements of 600 individual cells from WT and mutant strains were analyzed to
459 determine the frequency of motile cells during the observation period. Tracks from 50
460 individual motile cells corresponding to two min of observation and in six separate

461 experiments were analyzed to determine the gliding velocity and gliding motility
462 patterns.
463
464 **Quantitative plastic binding assay.** Frozen stocks of the WT and Δ*ftsZ* cells were
465 diluted in 1 ml of SP-4 medium to give a final concentration of approximately 10^7 CFU
466 ml^{-1}. The binding assay was performed as previously described (Burgos *et al.*, 2007).
467
468 **Haemadsorption (HA) activity.** For qualitative assessment of the HA, colonies grown
469 in SP4 plates were flooded with 2 ml of human erythrocytes diluted (1:50) in PBS and
470 incubated for 1 h at 37 °C. Plates were subsequently washed three times with PBS and
471 observed using a LeicaMZFLIII microscope. Pictures were taken using a LeicaDC500
472 camera connected to the microscope.
473
474 **Growth curves.** To compare the growth kinetics of WT and Δ*ftsZ* cells, two
475 independent experiments were performed using 48 cultures of 1 ml inoculated with
476 approximately 10^7 CFU ml^{-1} and grown in 24 well TPP plates at 37 ºC. ATP content
477 from six wells corresponding to each one of the different growth intervals was measured
478 using the ATP Bioluminescence Assay Kit HS II (Roche). Measuring ATP instead
479 of turbidity is considered the most proper method to estimate mycoplasma cell
480 mass (Lluch-Senar *et al.*, 2007; Stemke, 1995). Briefly, 1 ml of lysis reagent buffer
481 (Roche) was added to each well and 50 µl samples were then placed in Wallac B&W
482 isoplate polystyrene plates (Perkin Elmer). The ATP standard curve was constructed in
483 the range of 10^{-6} to 10^{-12} M. Standards and samples were measured by duplicate after
484 the automated injection of 50 µl of luciferase reagent in a Victor III luminometer
485 (Perkin Elmer) using SP-4 medium as blank. ATP concentrations were calculated from

a log-log plot of the standard curve data. The slopes corresponding to the exponential phase of growth were estimated from the linear regression of ATP values obtained from cultures grown for 0 h, 16 h, 24 h and 39 h. Mass doubling time of WT and Δ*ftsZ* was calculated from the slopes of the growth curves.

Obtaining and detecting non-adherent mutants. To detect spontaneous, non adherent phase variants, WT, Δ*ftsZ* and TnG*ftsZ* strains were grown in 25 cm^2 flasks with 5 ml of SP-4 medium inoculated with approximately 10^7 CFU ml^{-1}. After ~80 h the cultures were scraped off from the flasks and 2-ml samples of the suspensions were centrifuged to harvest cells, which were stored at -80 ºC for further DNA extraction. Successive passages were also performed in 25 cm^2 cell culture flasks with 5 ml of SP-4 that were inoculated with 50 µl of the cell suspension from the previous passage. The remaining of the cell suspension was passed through a 0.45 µm low binding protein filter (Millipore) and 300 µl samples of serial dilutions were spread on SP-4 plates, which were incubated 8 days at 37 °C. Plates showing 400-500 colonies (about 1,500 colonies per passage) were tested for haemadsorption as described above.

Quantitative PCR. The quantitative assay to detect the presence of recombinant chromosomes bearing deletions in the MgPa operon was performed using the LightCycler-FastStart DNA Master SYBR Green I (Roche) and the LightCycler.2 instrument (Roche). WT and Δ*ftsZ* genomic DNAs were used for two single-step PCR reactions using the R3-5' and R5-3' primers (Table S1) and primers mg281-5' and mg281-3'. R3-5' and R5-3' primers can detect the presence of a 558-bp DNA fragment (R3) resulting from the recombination between the MgPa operon and MgPa island VI (Fig. 5D) both in WT and Δ*ftsZ* genomes. Primers mg281-5' and mg281-3' amplify a

621-bp DNA fragment from *mg281* (T281) to quantify the number of *M. genitalium* genomes in the PCR reactions. The amplified fragments were detected by emission of fluorophore SYBR green at the 485-nm wavelength and the quantitative determination was carried out during the exponential phase of amplification. Multiple real-time data acquisition and analysis of the samples and of the known standard serial dilutions were performed and analyzed by MyiQ software (Roche). Dilutions of the known-titer standards (6.05×10^{13} molecules ml^{-1} for pBE-R3 and 4.13×10^{12} molecules ml^{-1} for pBE-T281; Table S2) were prepared in DEPC-H_2O, and 2 µl of each was used for the calibration curve in the amplification reaction. The calibration curves, obtained by quantification of the serial standard dilutions, were plotted in the dynamic range from 1.21×10^{4} to 12 molecules ml^{-1} for pBE-R3 and from 8.26×10^{6} to 8.26×10^{2} molecules ml^{-1} for pBE-T281. The concentration of the unknown-titer samples was obtained by interpolation on the calibration curve suggested by the software. A negative water control was added in each run to avoid overestimation of the specific product due to primer-dimer formation. Finally, the PCR amplification products were checked by agarose gel electrophoresis. Data in Fig. 5C are derived from five replicate Q-PCR measurements.

ACKNOWLEDGEMENTS

This work was supported by grant BIO2007-67904-C02-01 from the MCYT (Ministerio de Ciencia y Tecnología, Spain) to E.Q. and by the Centre de Referència de R+D de Biotecnologia (Generalitat de Catalunya). E.Q. is the Chair Holder of a "Cátedra de Transferencia de Tecnología Parc de Recerca UAB-Grupo Santander". M.L-S. acknowledges a FPI predoctoral fellowship from the MCYT. We acknowledge A.

535 Sánchez-Chardi for his advice in transmission electron microscopy and Drs. J. L.
536 Arolas, A. Mozo and L. Strother for their helpful comments.

537 Table 1. Parameters of WT and Δ*ftsZ* strains

Strain	% Non-adherent cells ± SE*	Doubling time (hours)	Cytokinesis length (hours)	Gliding velocity (μm s^{-1}) ± SE	Non-motile cells (%)	Haemadsorption§
WT	33.3 ± 4.2	11.9	1.07	0.146 ± 0.002	10	++
Δ*ftsZ*	34.7 ± 3.2	11.7	3.70	0.152 ± 0.003	39	++

538

539 * SE: standard error

540 § ++: all (Δ*ftsZ*) or most (WT) colonies in the HA assay were found to be evenly

541 covered with erythrocytes (Fig. 5A).

542 Table S1. Primers used in this study

Primer Name	Sequence (5'-3')
5'BEKOftsZ	CTGCAGAAAAGGTAGTTGTTGTTCTCGCTG
3'BEKOftsZ	GAATTCTTATTTAACCAAGCGTTGGAC
5'BDKOftsZ	GGATCCTTAATTTAATTTATCGTTTAGAATTGC
3'BDKOftsZ	ATCGATGAAGCAACTAAAGGGATAAAGAC
5'ftsZ	ATGGATGAAAATGA
3'ftsZ	TTAGTAGATTTGGTTTTGGTGCT
5'TnftsZ	CTCTGCAGTAGTATTTAGAATTAATAAAGTATGGATGAAAATGA
3'TnftsZ	GAATTCTTAGTAGATTTGGTTTTGGTGCT
RTmg225	TCTTATGCAGGGGTTGAAGATATC
R3-5'	ACCGGACCTAACCTTGATAG
R3-3'	GTAAAAATCTTATAAGAAGCAC
mg281-5'	GCATTTGACTTTTAATCAAAG
mg281-3'	GATTTCAACTTTACTTCTGC

543 Table S2. Plasmids used in this study

544

Plasmid	Source/Description
pBE	pBSKII+ derivative with MCS removed and substituted by a single *Eco*RV site (Pich *et al.*, 2006b).
pBE-BEftsZ	pBE derivative with a 1-kb fragment of the upstream region of the *ftsZ* gene cloned in the *Eco*RV site.
pBE-BDftsZ	pBE derivative with a 1-kb fragment of the downstream region of the *ftsZ* gene cloned in the *Eco*RV site.
MTn*TetM438*	Plasmid used to obtain the tetracycline resistance gene (Pich *et al.*, 2006b).
pΔftsZ*Tet*	Plasmid used to obtain the Δ*ftsZ* mutant.
pMTn*Gm*	Plasmid used to obtain pMTnG*ftsZ* (Pich *et al.*, 2006b).
pMTnG*ftsZ*	Plasmid derived from pMTn*Gm* containing the WT allele of the *ftsZ* gene.
pBE-R3	pBE derivative with a 558-bp fragment from the *M. genitalium* genome, which is the result of a recombination event between MgPa VI and the MgPa operon, and is cloned in the *Eco*RV site.
pBE-T281	pBE derivative with a 621-bp fragment of the *mg281* gene cloned in the *Eco*RV site.

545

Figure 1. Engineering of Δ*ftsZ* mutants.

A) Schematic representation of the double cross-over recombination event between pΔftsZ*Tet* and the homologous regions flanking *ftsZ*. DFR and UFR represent the downstream and upstream flanking regions of *mg224* in pΔftsZ*Tet*, respectively. The size of fragments resulting from the *Eco*RV (E) digestion of WT genomic DNA and the size of fragments resulting from the *Kpn*I (K) digestion of WT and Δ*ftsZ* genomic are indicated. S1 and S2 are the probes used in Southern blots B and F, respectively. Primers used in PCR reactions and RT-PCR are also shown with numbered arrows. P1: 5'BEKOftsZ; P2: 3'BEKOftsZ; P3: 5'ftsZ; P4: 3'ftsZ; P5: 5'RTmg225 and P6: 3'BDKOftsZ (Table S1). Additional restriction sites used for cloning: *Pst*I (P), *Eco*RI (E1), *Cla*I (C) and *Bam*HI (B).

B) Southern blot to demonstrate the replacement of *ftsZ* by the *tetM438* selectable marker. The 4.4-kb band was obtained by hybridizing the *Kpn*I digestion of Δ*ftsZ* genomic DNA with probe S1.

C) PCR detection of *ftsZ*. Lanes 1-3: PCR amplification using primers 5'ftsZ (P3) and 3'ftsZ (P4) and genomic DNAs of WT (lane 1) and the Δ*ftsZ* mutants obtained (lanes 2 and 3). Lanes 4-6: Positive controls of PCR amplifications using primers 5'BEΔftsZ (P1) and 3'BEΔftsZ (P2) and the same DNA templates used in lanes 1-3, respectively.

D) RT-PCR of *mg225* transcript in the WT and Δ*ftsZ* mutant. Total RNA from the *M. genitalium* G-37 (lane 2) and Δ*ftsZ* mutant (lane 4) was retrotranscribed using primer 3'BDKOftsZ (P6). The resulting cDNAs were amplified by PCR using primers 5'RTmg225 (P5) and 3'BDKOftsZ (P6), obtaining a fragment of 450 bp. The negative controls corresponding to the amplification by PCR of total RNAs from the WT and the Δ*ftsZ* mutant treated with DNase I are shown in lanes 1 and 3, respectively.

E) Southern blot to detect the presence of *ftsZ* and related sequences in the genome of the Δ*ftsZ* mutant. *Eco*RV-digested genomic DNAs from WT and Δ*ftsZ* (lanes 1 and 2, respectively) were hybridized with probe S2 (lanes 3 and 4, respectively). A 10.8-kb band is readily detected in lane 3 and has the size expected according to the *Eco*RV sites shown in panel A. No bands were observed in lane 4 even after an extended detection time.

Figure 2. Growth kinetics of WT and Δ*ftsZ* strains. Semi-logarithmic plot with the growth curves of WT (squares) and the Δ*ftsZ* mutant (triangles). Linear regression of ATP values from measures taken at 0 h, 16 h, 24 h and 39 h were used to determine the slopes corresponding to the exponential phase of growth. Error bars corresponding to the standard deviations of values obtained in three separate experiments are also represented.

Figure 3. Colony and cell morphology of WT and Δ*ftsZ* strains.

A) TEM images of the WT and Δ*ftsZ* strains. No significant differences are observed in the ultrastructure of the terminal organelle from cells of WT and Δ*ftsZ* strains (electrondense cores are marked with a black arrow). The white arrow highlights the presence of a tail on the opposite side to the terminal organelle frequently found in Δ*ftsZ* cells. Bar, 200 nm.

B) Colonies of WT and the Δ*ftsZ* mutant grown in culture dishes covered with SP-4 medium containing 0.5% low-melting-point agarose. Bar, 250 μm**.**

C) Selected frames from microcinematographies of WT and Δ*ftsZ* strains. The presence of many non-motile Δ*ftsZ* cells is indicated by white arrows. Most of these cells appear frequently coupled to another non-motile cell and both are linked by a thin filament. A

595 white circle indicates a single cell exhibiting a long filament. Bar, 5 μm. The complete
596 cinematographies can be found in supplementary material as Movie S1 and Movie S2,
597 respectively.
598
599 **Figure 4. Stages in the cell division process of WT, Δ*ftsZ* and TnG*ftsZ* strains.**
600 **A)** Histogram with the frequency of cells found in the different stages of cell division.
601 Δ*ftsZ* is indicated in black, WT in gray and in dark gray the complemented TnG*ftsZ*
602 strain. A picture with a representative cell from each stage is also shown. All pictures
603 are at the same magnification (bar, 500 nm). Stages: 1, individual cells exhibiting a
604 single terminal organelle and showing no tails in the opposite cell pole; 2, single cells
605 exhibiting two terminal organelles, one of them migrating to the opposite cell pole; 3,
606 dividing cells with two organelles in the opposite cell poles; 4, dividing cells with two
607 organelles in opposite cell poles but joined by a filament; 5, chains of filamented cells
608 and 6, individual cells exhibiting a single terminal organelle and showing long tails on
609 the opposite cell pole.
610 **B)** Representative SEM images of WT and Δ*ftsZ* cells. Cells in latter stages of cell
611 division are shown with white arrows. Individual cells after the division process with
612 long tails on the opposite side of the terminal organelle are circled in white. Bar, 5 μm.
613
614 **Figure 5. Quantification of non-adherent phase variants in serial culture passages.**
615 **A)** Pictures of representative colonies from WT and Δ*ftsZ* strains found after the HA
616 assay. All pictures are at the same magnification. Bar, 50 μm.
617 **B)** Frequency of HA^- colonies generated in serial passages. Black dots represent the
618 percentage of HA^- colonies in Δ*ftsZ* in the selected passages. Black squares show the
619 percentage of HA^- colonies from the WT strain.

620 **C)** Frequency of chromosomes bearing deletions in the MgPa operon in serial cultures
621 of WT (black squares) and Δ*ftsZ* (black dots). These recombinant genomes are the result
622 of a double cross-over between R3 and R5 boxes of MgPa VI island and the
623 homologous regions in the MgPa operon (see panel D). Frequencies are the average of
624 five replicate Q-PCR measurements and bars represent the respective standard errors.
625 **D)** Translocation of sequences from MgPa island VI to the MgPa operon in the *M.*
626 *genitalium* genome. Schematic representation of a reversible, double cross-over event
627 between the R3'-R3 and R5'-R5 boxes from the MgPa operon (bases 220,000 to
628 230,000) to MgPa island VI (bases 310,000 to 320,000). Boxes R1 to R6 refer to the
629 DNA repetitive sequences of the MgPa operon, which are also found in MgPa island VI
630 (R1' to R6') located 90 kb downstream. P1 and P2 indicate the position of the primers
631 used for Q-PCR. A number of additional double-recombination events are also possible
632 but are not included in the drawing for clarity. The location of the different MgPa
633 islands in the *M. genitalium* genome can be found in Lluch-Senar *et al*., (2007).

Supplementary Movie S1. Microcinematography showing gliding motility of WT cells. It is composed of 61 frames, each one taken at intervals of 2 s, and the resulting motion picture is shown at 10 frames s^{-1}. Labels 1-4 point to superimposed drawings of selected mycoplasma tracks (1, 3 and 4 show circular trajectories and 2 shows an erratic movement).

Supplementary Movie S2. Microcinematography showing gliding motility of Δ*ftsZ* cells. It is composed of 61 frames, each one taken at intervals of 2 s, and the resulting motion picture is shown at 10 frames s^{-1}. Labels 1-4 point to superimposed drawings of selected mycoplasma tracks (1 shows an erratic movement and 2-4 show circular trajectories). Cells connected by a thin filament are indicated by white arrows and cells exhibiting long filamented tails by red arrows.

Supplementary Figure S1. Complementation analyses of the Δ*ftsZ* mutant strain bearing a WT copy of the *ftsZ* allele (strain TnG*ftsZ*). A) Representative colonies grown in culture dishes covered with SP-4 medium containing 0.5% low-melting-point agarose (bar, 250 μm). B) Frequency of HA^- colonies generated in serial passages. C) Gliding parameters and haemadsorption properties. Data are compared with values from Table 1 of the main text. SE: standard error. A ++ symbol indicates that all (Δ*ftsZ*) or most (WT and TnG*ftsZ*) colonies in the haemadsorption assay were found to be evenly covered with erythrocytes (Fig. 5A).

REFERENCES

Alarcón, F., Vasconcelos, A.T.R.d., Yim, L., and Zaha, A. (2007) Genes involved in cell division in mycoplasmas. *Genetics and Molecular Biology* **30**: 174-181.

Benders, G.A., Powell, B.C., and Hutchison, C.A., 3rd (2005) Transcriptional analysis of the conserved *ftsZ* gene cluster in *Mycoplasma genitalium* and *Mycoplasma pneumoniae*. *J Bacteriol* **187**: 4542-4551.

Bredt, W. (1968) Motility and multiplication of *Mycoplasma pneumoniae*. A phase contrast study. *Pathol Microbiol (Basel)* **32**: 321-326.

Burgos, R., Pich, O.Q., Ferrer-Navarro, M., Baseman, J.B., Querol, E., and Pinol, J. (2006) *Mycoplasma genitalium* P140 and P110 cytadhesins are reciprocally stabilized and required for cell adhesion and terminal-organelle development. *J Bacteriol* **188**: 8627-8637.

Burgos, R., Pich, O.Q., Querol, E., and Pinol, J. (2007) Functional analysis of the *Mycoplasma genitalium* MG312 protein reveals a specific requirement of the MG312 N-terminal domain for gliding motility. *J Bacteriol* **189**: 7014-7023.

Burgos, R., Pich, O.Q., Querol, E., and Pinol, J. (2008) Deletion of the *Mycoplasma genitalium* MG_217 gene modifies cell gliding behaviour by altering terminal organelle curvature. *Mol Microbiol* **69**: 1029-1040.

Cohen, C.R., Nosek, M., Meier, A., Astete, S.G., Iverson-Cabral, S., Mugo, N.R., and Totten, P.A. (2007) *Mycoplasma genitalium* infection and persistence in a cohort of female sex workers in Nairobi, Kenya. *Sex Transm Dis* **34**: 274-279.

Fraser, C.M., Gocayne, J.D., White, O., Adams, M.D., Clayton, R.A., Fleischmann, R.D., Bult, C.J., Kerlavage, A.R., Sutton, G., Kelley, J.M., Fritchman, R.D., Weidman, J.F., Small, K.V., Sandusky, M., Fuhrmann, J., Nguyen, D., Utterback, T.R., Saudek, D.M., Phillips, C.A., Merrick, J.M., Tomb, J.F., Dougherty, B.A., Bott, K.F., Hu, P.C., Lucier, T.S., Peterson, S.N., Smith, H.O., Hutchison, C.A., 3rd, and Venter, J.C. (1995) The minimal gene complement of *Mycoplasma genitalium*. *Science* **270**: 397-403.

French, C.T., Lao, P., Loraine, A.E., Matthews, B.T., Yu, H., and Dybvig, K. (2008) Large-Scale Transposon Mutagenesis of *Mycoplasma pulmonis*. *Mol Microbiol*.

Glass, J.I., Assad-Garcia, N., Alperovich, N., Yooseph, S., Lewis, M.R., Maruf, M., Hutchison, C.A., 3rd, Smith, H.O., and Venter, J.C. (2006) Essential genes of a minimal bacterium. *Proc Natl Acad Sci U S A* **103**: 425-430.

Hasselbring, B.M., Jordan, J.L., Krause, R.W., and Krause, D.C. (2006a) Terminal organelle development in the cell wall-less bacterium *Mycoplasma pneumoniae*. *Proc Natl Acad Sci U S A* **103**: 16478-16483.

Hasselbring, B.M., Page, C.A., Sheppard, E.S., and Krause, D.C. (2006b) Transposon mutagenesis identifies genes associated with *Mycoplasma pneumoniae* gliding motility. *J Bacteriol* **188**: 6335-6345.

Hasselbring, B.M., and Krause, D.C. (2007) Proteins P24 and P41 function in the regulation of terminal-organelle development and gliding motility in *Mycoplasma pneumoniae*. *J Bacteriol* **189**: 7442-7449.

Hatchel, J.M., and Balish, M.F. (2008) Attachment organelle ultrastructure correlates with phylogeny, not gliding motility properties, in *Mycoplasma pneumoniae* relatives. *Microbiology* **154**: 286-295.

Hjorth, S.V., Bjornelius, E., Lidbrink, P., Falk, L., Dohn, B., Berthelsen, L., Ma, L., Martin, D.H., and Jensen, J.S. (2006) Sequence-based typing of *Mycoplasma genitalium* reveals sexual transmission. *J Clin Microbiol* **44**: 2078-2083.

Hottes, A.K., Shapiro, L., and McAdams, H.H. (2005) DnaA coordinates replication initiation and cell cycle transcription in *Caulobacter crescentus*. *Mol Microbiol* **58**: 1340-1353.

Hutchison, C.A., Peterson, S.N., Gill, S.R., Cline, R.T., White, O., Fraser, C.M., Smith, H.O., and Venter, J.C. (1999) Global transposon mutagenesis and a minimal *Mycoplasma* genome. *Science* **286**: 2165-2169.

Iverson-Cabral, S.L., Astete, S.G., Cohen, C.R., and Totten, P.A. (2007) mgpB and mgpC sequence diversity in *Mycoplasma genitalium* is generated by segmental reciprocal recombination with repetitive chromosomal sequences. *Mol Microbiol* **66**: 55-73.

Jensen, J.S., Blom, J., and Lind, K. (1994) Intracellular location of *Mycoplasma genitalium* in cultured Vero cells as demonstrated by electron microscopy. *Int J Exp Pathol* **75**: 91-98.

Jensen, J.S. (2004) *Mycoplasma genitalium*: the aetiological agent of urethritis and other sexually transmitted diseases. *J Eur Acad Dermatol Venereol* **18**: 1-11.

Jensen, R.B. (2006) Coordination between chromosome replication, segregation, and cell division in *Caulobacter crescentus*. *J Bacteriol* **188**: 2244-2253.

Krause, D.C., and Balish, M.F. (2001) Structure, function, and assembly of the terminal organelle of *Mycoplasma pneumoniae*. *FEMS Microbiol Lett* **198**: 1-7.

Leaver, M., Dominguez-Cuevas, P., Coxhead, J.M., Daniel, R.A., and Errington, J. (2009) Life without a wall or division machine in *Bacillus subtilis*. *Nature* **457**: 849-853.

Lluch-Senar, M., Vallmitjana, M., Querol, E., and Pinol, J. (2007) A new promoterless reporter vector reveals antisense transcription in *Mycoplasma genitalium*. *Microbiology* **153**: 2743-2752.

Ma, L., Jensen, J.S., Myers, L., Burnett, J., Welch, M., Jia, Q., and Martin, D.H. (2007) *Mycoplasma genitalium*: an efficient strategy to generate genetic variation from a minimal genome. *Mol Microbiol* **66**: 220-236.

McGowin, C.L., Popov, V.L., and Pyles, R.B. (2009) Intracellular *Mycoplasma genitalium* infection of human vaginal and cervical epithelial cells elicits distinct patterns of inflammatory cytokine secretion and provides a possible survival niche against macrophage-mediated killing. *BMC Microbiol* **9**: 139.

Mernaugh, G.R., Dallo, S.F., Holt, S.C., and Baseman, J.B. (1993) Properties of adhering and nonadhering populations of *Mycoplasma genitalium*. *Clin Infect Dis* **17 Suppl 1**: S69-78.

Peterson, S.N., Bailey, C.C., Jensen, J.S., Borre, M.B., King, E.S., Bott, K.F., and Hutchison, C.A., 3rd (1995) Characterization of repetitive DNA in the *Mycoplasma genitalium* genome: possible role in the generation of antigenic variation. *Proc Natl Acad Sci U S A* **92**: 11829-11833.

Pich, O.Q., Burgos, R., Ferrer-Navarro, M., Querol, E., and Pinol, J. (2006a) *Mycoplasma genitalium mg200* and *mg386* genes are involved in gliding motility but not in cytadherence. *Mol Microbiol* **60**: 1509-1519.

Pich, O.Q., Burgos, R., Planell, R., Querol, E., and Pinol, J. (2006b) Comparative analysis of antibiotic resistance gene markers in *Mycoplasma genitalium*: application to studies of the minimal gene complement. *Microbiology* **152**: 519-527.

Pich, O.Q., Burgos, R., Ferrer-Navarro, M., Querol, E., and Pinol, J. (2008) Role of *Mycoplasma genitalium* MG218 and MG317 cytoskeletal proteins in terminal organelle organization, gliding motility and cytadherence. *Microbiology* **154**: 3188-3198.

Ramsby, M.L., and Makovsky, G.S. (1999) Differential detergent fractionation of eukaryotic cells. Analysis by two-dimensional gel electrophoresis. 2-D Proteome Analysis Protocols. *Methods in Molecular Biology* **112**.

Regula, J.T., Boguth, G., Gorg, A., Hegermann, J., Mayer, F., Frank, R., and Herrmann, R. (2001) Defining the mycoplasma 'cytoskeleton': the protein composition of the Triton X-100 insoluble fraction of the bacterium *Mycoplasma pneumoniae* determined by 2-D gel electrophoresis and mass spectrometry. *Microbiology* **147**: 1045-1057.

Rothfield, L., Taghbalout, A., and Shih, Y.L. (2005) Spatial control of bacterial division-site placement. *Nat Rev Microbiol* **3**: 959-968.

Shen, X., Collier, J., Dill, D., Shapiro, L., Horowitz, M., and McAdams, H.H. (2008) Architecture and inherent robustness of a bacterial cell-cycle control system. *Proc Natl Acad Sci U S A* **105**: 11340-11345.

Stemke, J.A.R.a.G.W. (1995) Measurement of Mollicute Growth bt ATP-Dependent Luminometry. In *Molecular and Diagnostic Procedures in Mycoplasmology*. Vol. I. Razin, S. and Tully, J.G. (eds). San Diego, California: Academic press, INC., pp. 65-71.

Tully, J.G., Rose, D.L., Whitcomb, R.F., and Wenzel, R.P. (1979) Enhanced isolation of *Mycoplasma pneumoniae* from throat washings with a newly-modified culture medium. *J Infect Dis* **139**: 478-482.

Weisburg, W.G., Tully, J.G., Rose, D.L., Petzel, J.P., Oyaizu, H., Yang, D., Mandelco, L., Sechrest, J., Lawrence, T.G., Van Etten, J., and et al. (1989) A phylogenetic analysis of the mycoplasmas: basis for their classification. *J Bacteriol* **171**: 6455-6467.

Weiss, D.S. (2004) Bacterial cell division and the septal ring. *Mol Microbiol* **54**: 588-597.

Figure 1

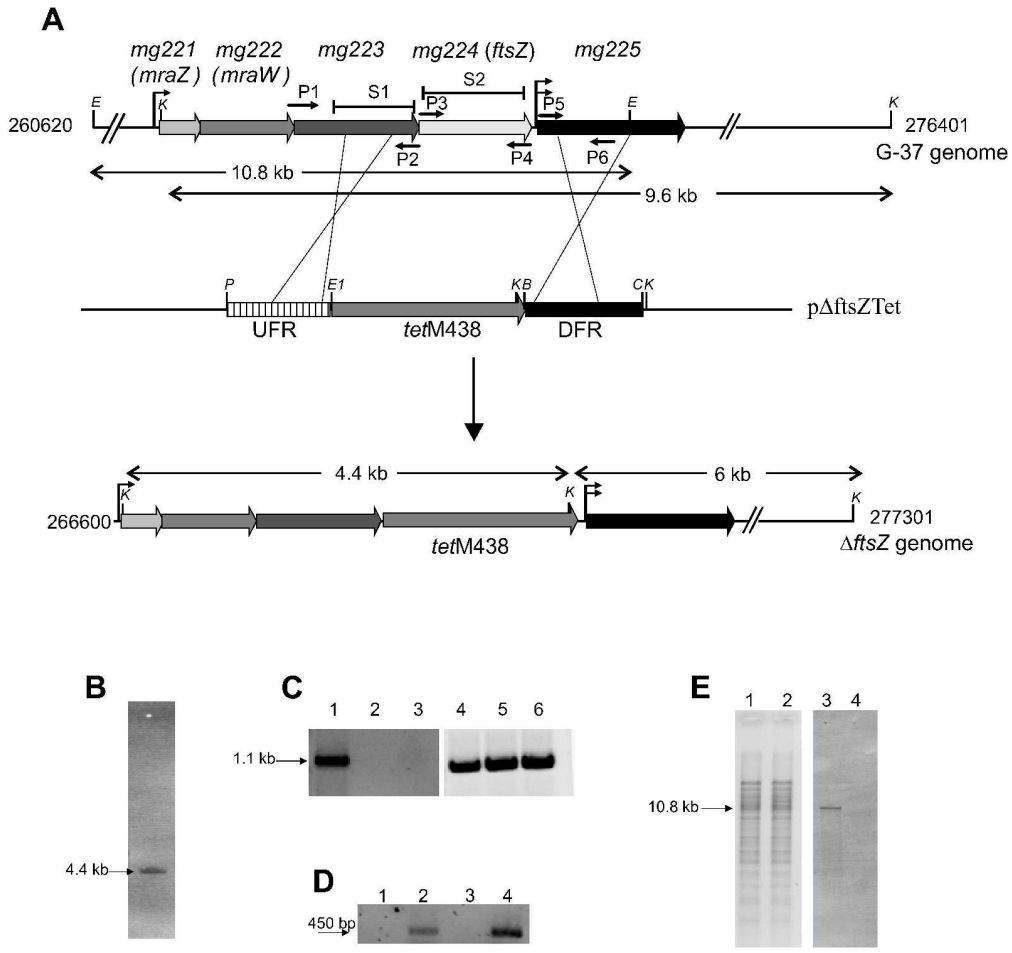

135x156mm (600 x 600 DPI)

Figure 2

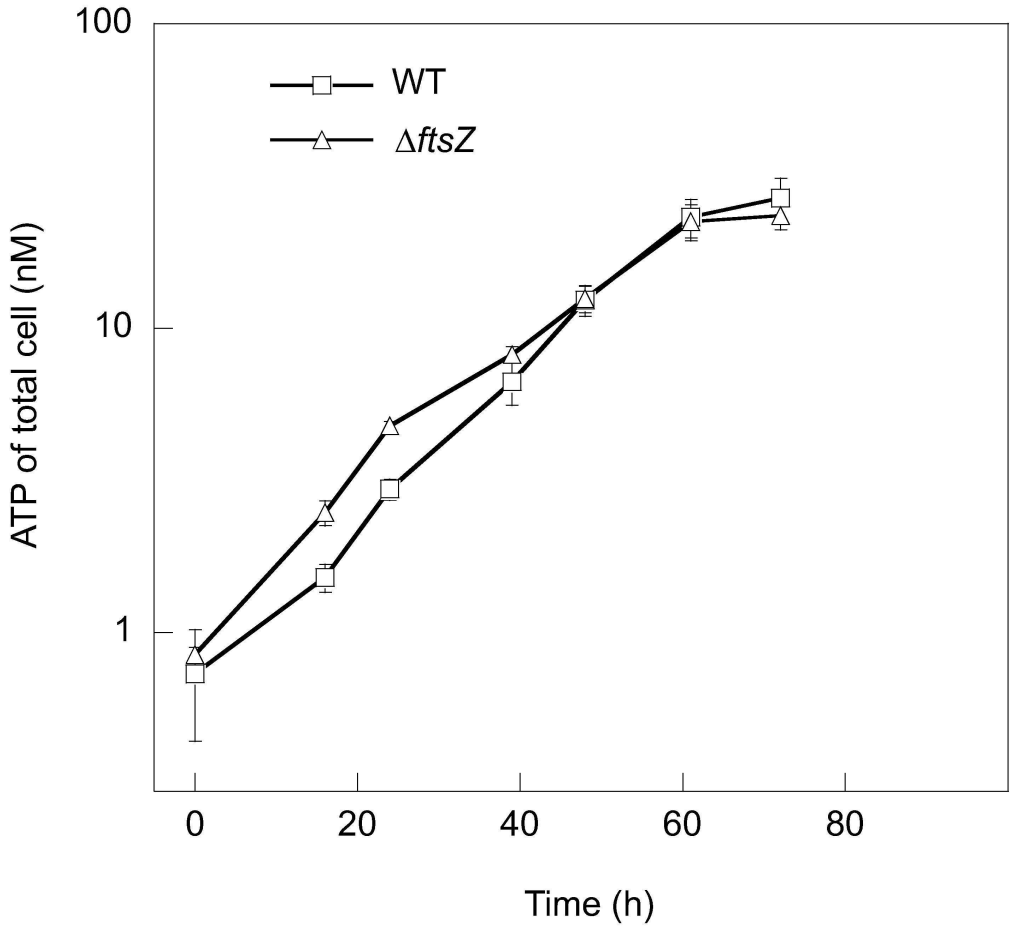

119x137mm (600 x 600 DPI)

Figure 3

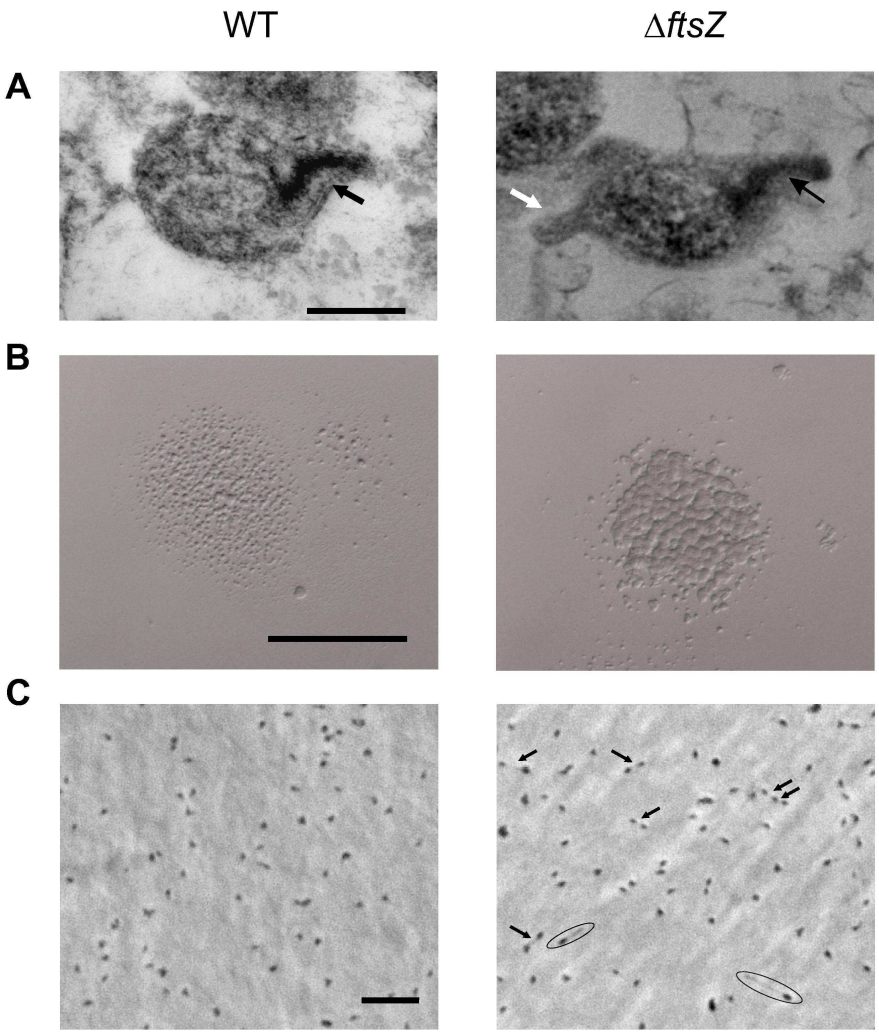

110x151mm (600 x 600 DPI)

Figure 4

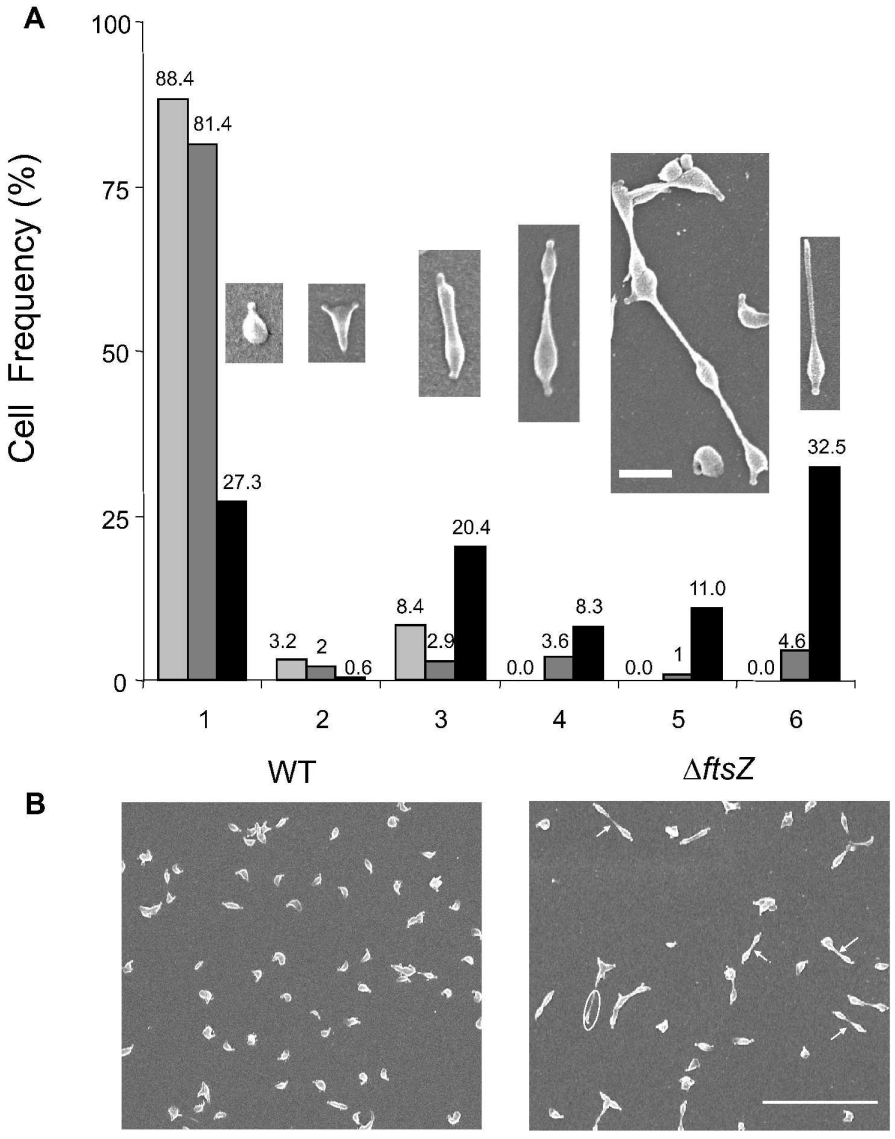

125x168mm (600 x 600 DPI)

Figure 5

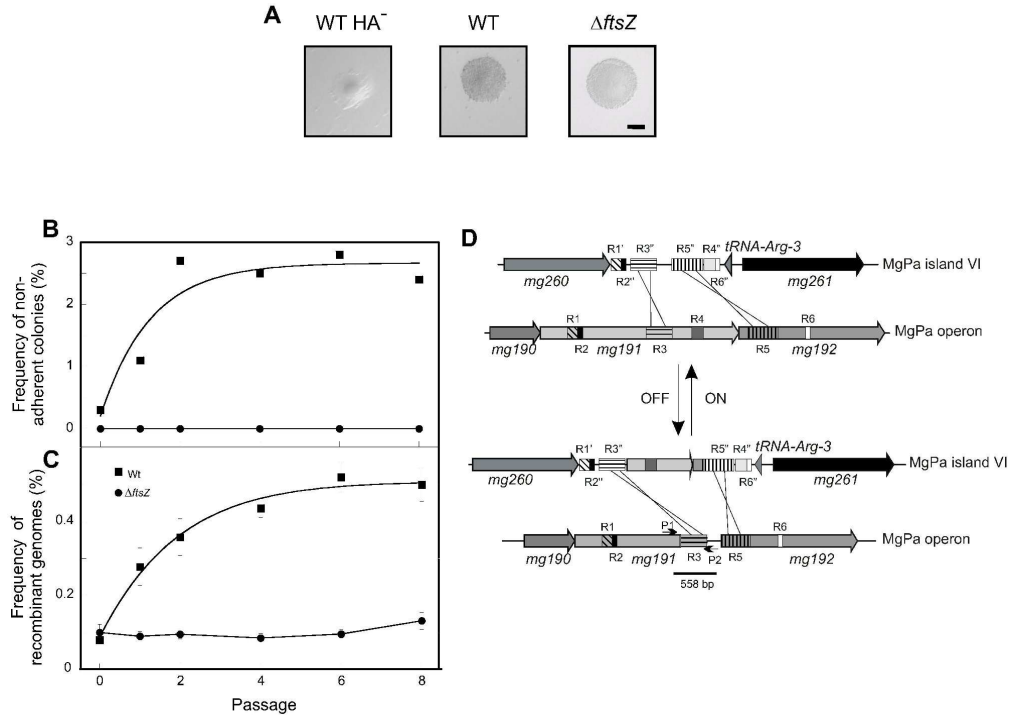

168x164mm (600 x 600 DPI)

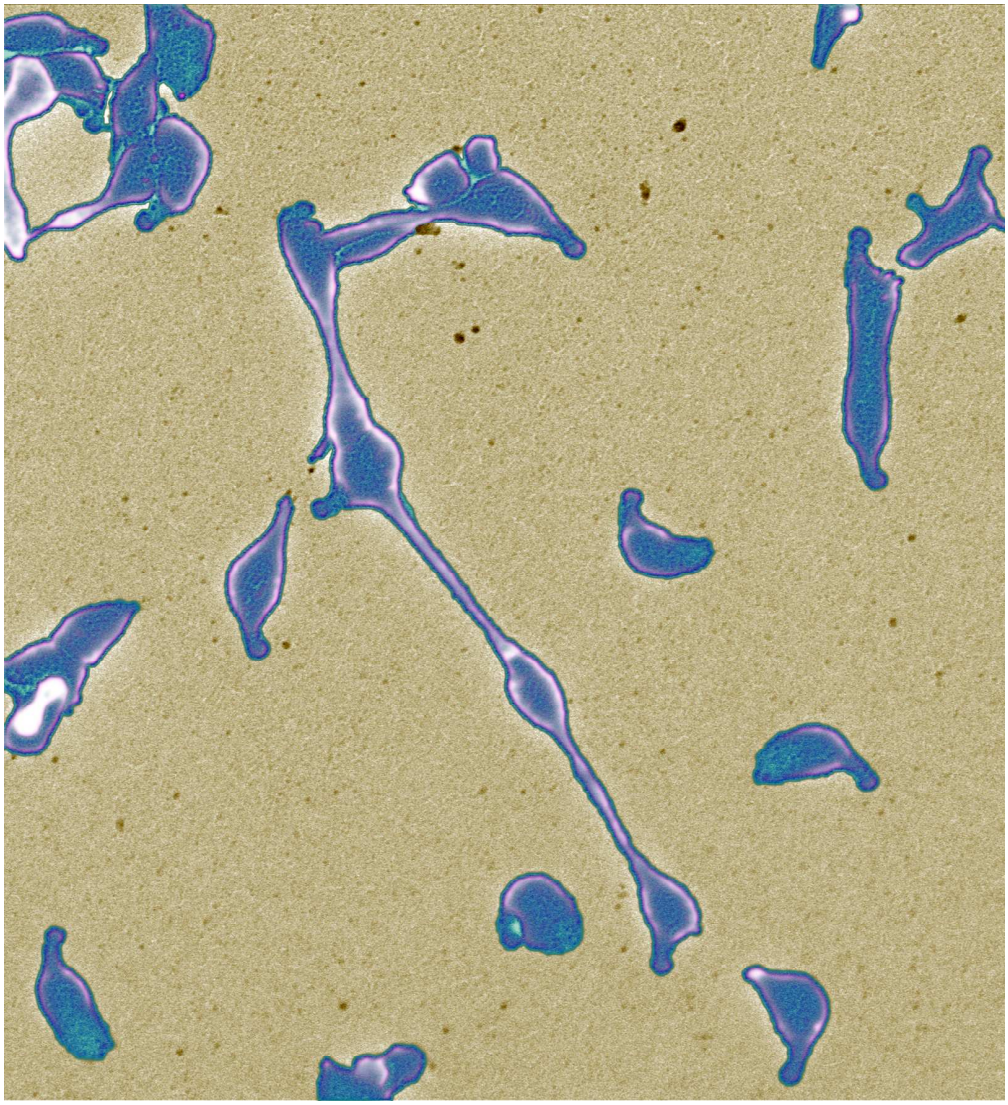

205x224mm (600 x 600 DPI)